# Moderate plasma activated media suppresses proliferation and migration of MDCK epithelial cells

You may also be interested in:

# Moderate plasma activated media suppresses proliferation and migration of MDCK epithelial cells

**Soheila Mohades**[1]**, Mounir Laroussi**[1] **and Venkat Maruthamuthu**[2]

[1] Plasma Engineering and Medicine Institute, Old Dominion University, Norfolk, VA 23529,
United States of America
[2] Department of Mechanical and Aerospace Engineering, Old Dominion University, Norfolk, VA 23529,
United States of America

E-mail: mlarouss@odu.edu

## Abstract

Low-temperature plasma has been shown to have diverse biomedical uses, including its applications in cancer and wound healing. One recent approach in treating mammalian cells with plasma is through the use of plasma activated media (PAM), which is produced by exposing cell culture media to plasma. While the adverse effects of PAM treatment on cancerous epithelial cell lines have been recently studied, much less is known about the interaction of PAM with normal epithelial cells. In this paper, non-cancerous canine kidney MDCK (Madin-Darby Canine Kidney) epithelial cells were treated by PAM and time-lapse microscopy was used to directly monitor their proliferation and random migration upon treatment. While longer durations of PAM treatment led to cell death, we found that moderate levels of PAM treatment inhibited proliferation in these epithelial cells. We also found that PAM treatment reduced random cell migration within epithelial islands. Immunofluorescence staining showed that while there were no major changes in the actin/adhesion apparatus, there was a significant change in the nuclear localization of proliferation marker Ki-67, consistent with our time-lapse results.

Keywords: low temperature plasma, cell proliferation, cell migration, plasma activated media, time-lapse microscopy, immunofluorescence, Ki-67

S Supplementary material for this article is available online

(Some figures may appear in colour only in the online journal)

## 1. Introduction

Low temperature plasma (LTP) is a weakly ionized gas, composed of electrons, ions, chemically reactive (and non-reactive) species and radicals where the heavy particles (ions and neutrals) remain at low energy. LTP has multiple applications in biology and medicine such as inactivation of micro-organisms [1, 2], dental disinfection [3], wound healing [4], and cancer therapy [5, 6]. Understanding the interactions of plasma with mammalian cells is critically important for anti-cancer and wound healing applications. Key cell biological processes that may be impacted in these applications include cell proliferation, death, and migration.

Several studies have documented the effects of treating cells, especially cancerous ones, by plasma [7]. Different approaches have been taken in treating cells with LTP including direct exposure to plasma or using plasma activated media (PAM) [8–13]. PAM provides distinct advantages such as the isolation of the effects of chemical species in the activated media from the direct effects of plasma's other agents such as charged particles, UV radiation, and heat. PAM also allows storage for later use. It has been revealed that reactive oxygen spices (ROS)
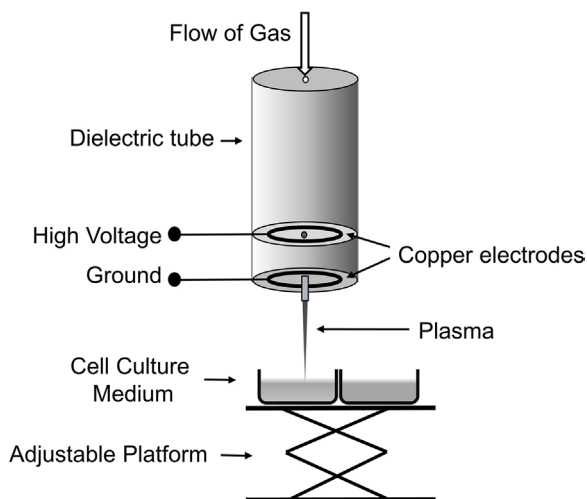
1361-6463/17/185205+9$33.00

1

J. Phys. D: Appl. Phys. **50** (2017) 185205

S Mohades *et al*



**Figure 1.** Schematic of the plasma pencil used for the preparation of plasma activated media.

and reactive nitrogen spices (RNS) are primarily responsible for the biomedical impacts of LTP involving macromolecular damage such as peroxidation of lipids and induction of DNA damage [14–17]. Ultimately, a sufficiently high dose of such oxidative stress resulted in cell death via necrosis or apoptosis in cancer or normal cells [18–20]. The impact of LTP on cell migration is also important due to its role in tumor metastasis, wound repair, and angiogenesis [21]. Plasma treatment has been shown to reduce single cell migration rate and induce cell detachment by reducing integrin expression [22, 23]. Results of a migration assay showed that plasma treatment reduces cell migration and proliferation in a scratched monolayer of cells [24, 25]. Plasma was also shown to have anti-proliferation effects on a multicellular tumor spheroid [26].

Most current cancer therapy methods are associated with unwanted side effects due to damage of normal cells and healthy tissues. Although the cross section of the plasma plume in a plasma jet device is small and the treatment area is localized, it is very important to understand the interaction of plasma with normal cells. Prior research indicates that normal cells are more resistant to oxidative stress than cancer cells and it has been reported that plasma treatment can be used to selectively treat some cell types [27–29]. For example, Fridman *et al* reported the absence of skin damage induced by plasma treatment [30]. It is important to mention here that the selective effect of plasma treatment is highly dependent on the dose (time) of plasma exposure. Normal cells can survive a moderate level of oxidative stress but a longer exposure time can induce severe irreversible damage [31].

In this paper, we use non-cancerous canine kidney epithelial cells to evaluate the effects of PAM on normal epithelial cells with respect to the fundamental processes of cell proliferation, adhesion, and migration. We used time-lapse cell microscopy to directly observe cell proliferation, death, and migration. We also used immunofluorescence to observe markers of cell adhesion and proliferation in control and PAM treated samples. Our results indicate a clear mitigation of proliferation as well as a reduction in random cell migration within epithelial islands.

## 2. Experimental methods

### 2.1. Plasma source and PAM

The source of LTP used in this work is the plasma pencil which is shown schematically in figure 1. The plasma pencil is composed of two ring-shaped electrodes embedded in perforated disks and located parallel to each other at a distance variable from 0.5 to 1 cm. More details of the plasma pencil can be found in [32]. Plasma is ignited by applying a pulsed high voltage and a flow of helium gas with 99.99% purity. For all experiments, plasma was operated with the following conditions unless otherwise mentioned: a frequency of 5 kHz, voltage of 7 kV, pulse width of 800 ns, and a flow rate of $5.0 \pm 0.1$ slm. The distance between the tip of the nozzle and surface of media in the cell culture dish was ~22 mm.

To prepare PAM, 1 ml of Eagle's Minimum Essential Medium (EMEM) complete cell culture media (supplemented with 10% Bovine Calf Serum and 1% Penicillin/Streptomycin/Glutamine) was added in each well of a 24-well plate and was exposed to the plasma pencil for the desired exposure times. The pH and temperature of PAM were measured before and after plasma exposure and results indicated that plasma treatment does not change either of these (data not shown).

### 2.2. Cell culture

MDCK (ATCC® CCL-34™) cells were cultured in EMEM (ATCC, Manassas, VA) supplemented with 10% Bovine Calf Serum and 1% Penicillin/Streptomycin/Glutamine purchased from HyClone (Logan, UT, USA) as recommended by the provider (ATCC, Manassas, VA). MDCK cells are normal (non-cancerous) epithelial cells originally derived from a canine kidney. Cells were seeded in a 75 cm$^2$ vented cell culture flasks and stored at 37 °C in a humidified incubator with 5% $CO_2$ for 3 d or once cells had reached a high confluence. Then, a cell suspension with a desired density was prepared and seeded into either a 96-well, 24-well, or 6-well plate depending on the experimental protocol (as stated in the following sections). Plates were incubated overnight at 37 °C in a humidified incubator with 5% $CO_2$ before treatment with PAM.

### 2.3. PAM treatment of cells and the cell viability assay

To evaluate the effect of PAM treatment on net MDCK cell number, the CellTiter 96® AQueous One Solution Cell Proliferation Assay (MTS) (Promega, Madison, MI, USA) was employed. In this assay, metabolically active cells reduce the MTS tetrazolium compound into a colourful formazan product that is measurable using absorbance detection with a microplate reader. In this protocol, MDCK cells were seeded in a 96-well plate at a cell density of $2 \times 10^4$ cells/well and were incubated overnight at 37 °C in a humidified incubator with 5% $CO_2$. For PAM treatment, the older media on cells were replaced with 100 $\mu$l of PAM which was prepared by 2, 3, 4, 6, and 10 min plasma exposure. The control sample was treated with fresh complete cell culture media without plasma exposure. Then, cells were stored in an incubator for
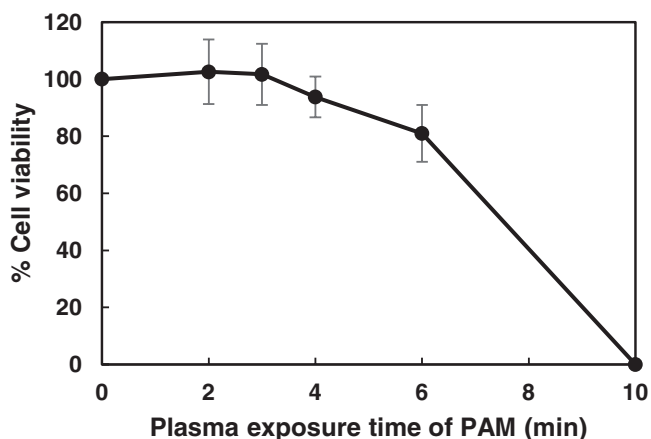
J. Phys. D: Appl. Phys. 50 (2017) 185205

S Mohades *et al*



**Figure 2.** Effects of PAM on the viability of MDCK epithelial cells using MTS assay at 48 h of PAM treatment. The percentage of metabolically active cells was normalized to the control. Results are shown from three independent experiments with two replications, as mean $\pm$ SD (standard deviation).

delayed cell viability measurements at 12, 24, and 48 h post-PAM application. At each measurement time, 20 $\mu$l of the MTS solution was added to 100 $\mu$l of freshly replaced cell culture media in each sample well of the 96-well plate and incubated for 1 h at 37 °C. Absorbance was measured at 490 nm using a microplate reader (AgileReader, ACTGene Inc.). All experiments were conducted as three sets of independent experiments and the results are expressed as the number of metabolically active cells per ml. Trypan blue exclusion assay was used to quantify the data achieved from the MTS assay. In this dye exclusion assay, live cells exclude the trypan blue dye and remain unstained while dead cells uptake the dye in and turn blue because of their damaged cell membrane.

### 2.4. Time-lapse imaging

Time-lapse imaging was used to monitor changes in cells during PAM treatment. Here, MDCK cells were seeded at $8 \times 10^4$ cells per well in a 24-well plate overnight. Then, 2 portions of 5 min PAM (1 ml each), as explained in section 2.1, were used to treat the cells. Media was buffered with 10 mM HEPES solution to stabilize the pH during imaging. Since PAM with lower exposure time (3 min or below) did not induce a noticeable change in cell viability of MDCK cells and very long exposure times such as 10 min PAM caused severe cell death, 5 min plasma exposure was selected to provide PAM of moderate intensity (refer to cell viability results of PAM shown in figure 2). Right after PAM application, time-lapse microscopy of PAM and control samples was started. The 24-well plate was fixed on an automated stage at an ambient temperature of 37 °C. Phase-contrast images were acquired at 10$\times$ magnification using an inverted microscope (DMi8, Leica Microsystems) equipped with a CCD camera (Andor Technology Ltd). Images were captured every 10 min for a period of 48 h (288 images) of PAM treatment. ImageJ software (NIH) was used for the processing and analysis of the resulting images.

### 2.5. Immunofluorescence

For immunofluorescence experiments, $8 \times 10^4$ cells per well of MDCK cells were grown overnight on collagen coated (0.2 mg ml$^{-1}$ col1) square coverslips which were placed in a 6-well plate. Cells were then treated with 2 portions (1 ml each) of 5 min PAM in addition to 1 ml of the fresh complete cell culture media. For the control samples, the older media was replaced by 3 ml of fresh complete cell culture media. Cells were incubated for 48 h at 37 °C in a humidified incubator with 5% $CO_2$. Then, the media were discarded and coverslips were washed with CB buffer (Cytoskeletal buffer: 10 mM MES, 3 mM $MgCl_2$, 0.14 M KCl, pH 6.8). This was followed by a 15 min incubation in a permeabilization/fixing solution containing 4% paraformaldehyde, 1.5% BSA and 0.5% Triton in CB buffer at room temperature. Cells were then washed three times with PBS, for 5 min each time. Samples were then incubated in an appropriate dilution of each of the primary antibodies or 488-phalloidin for 1 h, followed by three PBS washes and were then incubated for 1 h with the secondary antibodies. Then, after a PBS wash, cells were incubated in DAPI (4′,6-Diamidino-2-Phenylindole) diluted in PBS for 5 min. Each coverslip was mounted on a glass slide and stored overnight at 4 °C prior to imaging. Fluorescence images of cells were acquired using an epi-fluorescence microscope (DMi8, Leica Microsystems) equipped with a CCD camera (Andor Technology Ltd) and 10$\times$, 20$\times$, and 40$\times$ objectives. All chemicals used for immunofluorescence were from Fisher Scientific unless mentioned otherwise. The following primary antibodies were used: anti-beta-catenin (BD Biosciences) to mark cell–cell adhesions, anti-paxillin (Santa Cruz Biotech) to mark cell-surface adhesions and anti-Ki-67 (Dako) to mark proliferating cell nuclei. Anti-beta-catenin and anti-paxillin antibodies were used at 1:100 dilution and anti-Ki-67 was used at 1:150 dilution. Phalloidin-488 (Molecular Probes) was used at 1:200 dilution to mark filamentous actin. The secondary antibodies used were anti-mouse and anti-rabbit IgG (Jackson ImmunoResearch), both used at 1:200 dilution.

### 2.6. Statistical methods

All experiments were repeated at least three times. Statistical analyses were performed using SPSS software (IBM, USA). Results were analyzed using chi-square test or independent $t$-test as stated in the results. A $p$-value below 0.05 was considered to be statistically significant ($^*$ denotes $p < 0.05$, $^{**}$ denotes $p < 0.01$ and $^{***}$ denotes $p < 0.001$).

## 3. Results and discussion

### 3.1. Effects of PAM treatment on viability of MDCK cells

We first used the MTS assay to determine the effect of PAM treatment on MDCK cell viability with PAM generated for various plasma exposure times. The MTS assay (taken together with the trypan blue exclusion assay) yields the number of live cells at a given time point. Figure 2 shows the
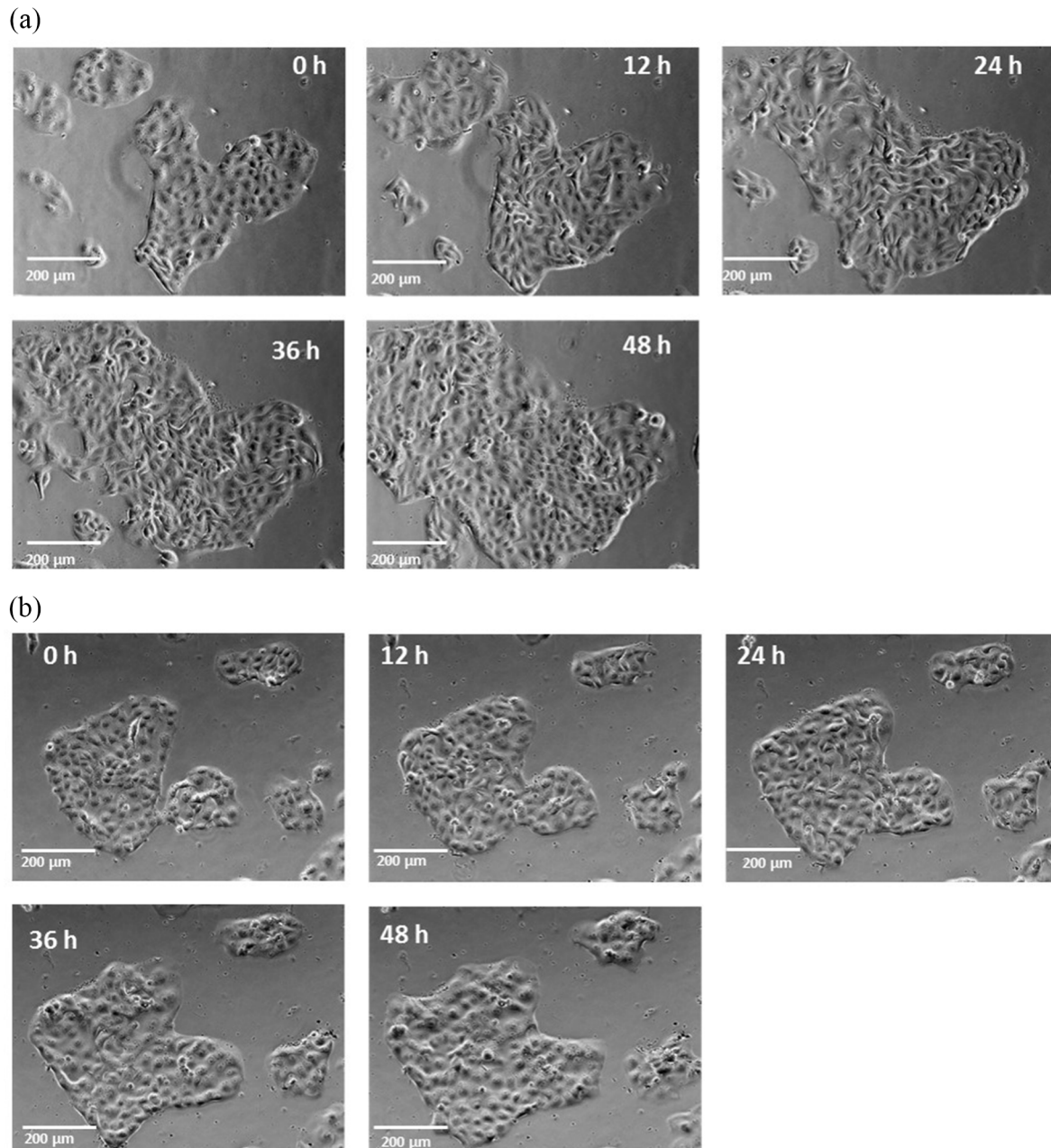
J. Phys. D: Appl. Phys. **50** (2017) 185205

S Mohades *et al*

(a)



(b)



**Figure 3.** Phase contrast images of (a) control and (b) PAM treated MDCK cells obtained by time-lapse microscopy at different time points of 0, 12, 24, 36, 48 h show a significant increase in cell population in the control sample compared to the PAM treated sample. Scale bar: 200 $\mu$m.

results of the MTS assay at 48 h after PAM initiation. Here, the percentage cell viability, defined as the live cell number normalized with respect to the control case of no PAM treatment, has been plotted as a function of PAM level which we define as the duration of LTP exposure time (min) to make PAM. While PAM with up to 3 min plasma exposure time did not show a difference in percentage cell viability after 48 h, PAM with greater exposure times showed a progressive decrease in cell number. For instance, 6 min PAM treatment resulted in 20% cell viability reduction. Eventually, 10 min PAM induces widespread cell death leaving no metabolically active cells.

This data suggests that PAM with moderate exposure times, such as around 5 min leads to a reduction in cell number, while avoiding widespread cell death as in the 10 min PAM sample. Thus, PAM with 5 min plasma exposure (moderate level of PAM treatment) was chosen for the rest of the study, in order to ascertain if cell death alone was leading to reduced cell numbers or whether there was an impact of PAM on the proliferation of MDCK cells. Note that this trend is different from what we observed in PAM treatment of squamous cell carcinoma of urinary bladder (SCaBER) which indicated a more than 90% cell death after a 4 min PAM treatment. The effect of PAM and aged-PAM on SCaBER cells and its correlation with the concentration of hydrogen peroxide generated in the media were published recently in [27].
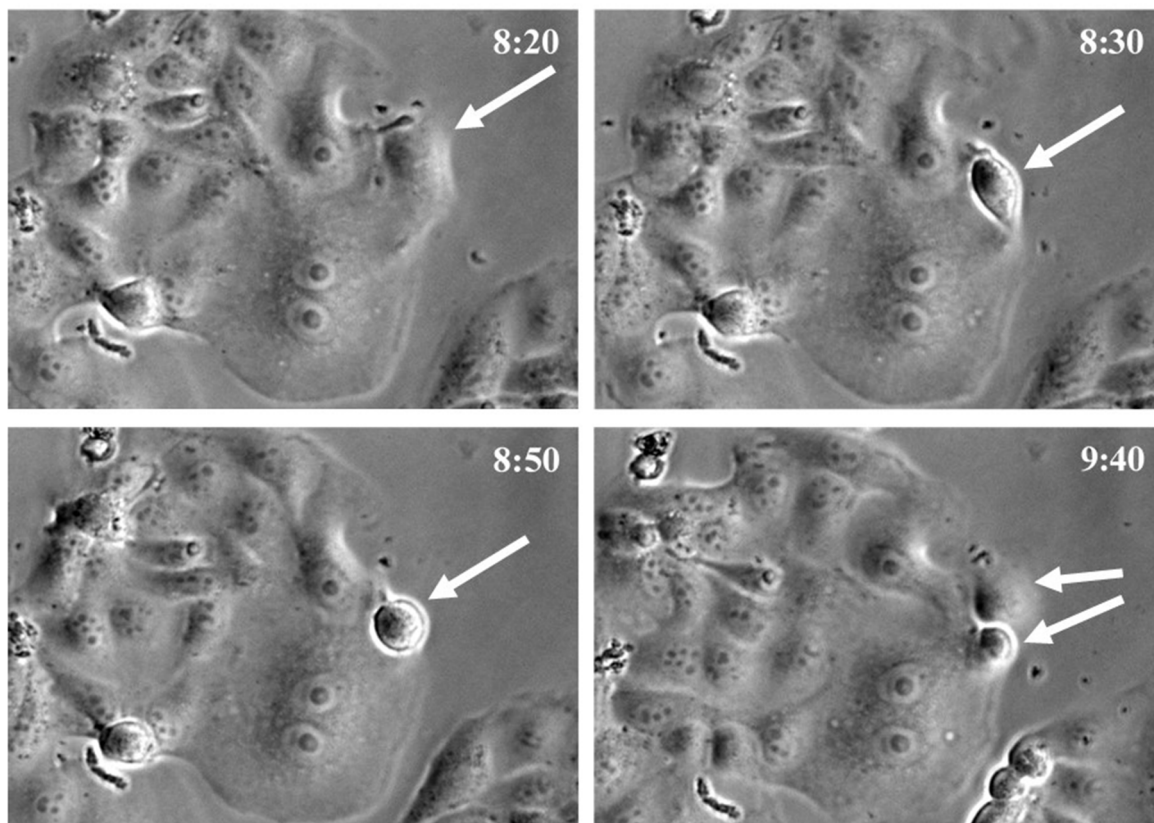
**Figure 4.** Phase-contrast images obtained from time-lapse imaging (of control sample) show reshaping of a dividing cell (white arrow) which adopts a round morphology from a spread shape and the re-spreading of daughter cells after cell division. Time is indicated in hour:min.

### 3.2. Time-lapse phase imaging upon PAM treatment

In order to ascertain the effect of moderate PAM treatment on MDCK cell morphology, proliferation, and migration in PAM and control samples, we carried out time-lapse phase imaging of the cells upon PAM treatment. In these experiments, phase images of cells were taken every 10 min during the 48 h following PAM treatment initiation. Figure 3 shows images of the control and PAM treated samples respectively at 0, 12, 24, 36, and 48 h. These images are selected from time-lapse movies that are provided as online supplementary material (stacks.iop.org/JPhysD/50/185205/mmedia) (available from link). Figure 3(a) and the supplementary movie 1 of the control sample demonstrates rapid proliferation in cells over 48 h. In contrast, cells in the PAM treated sample did not show a similar increase in population number which is visually clear in figure 3(b) and in the supplementary movie 2 of the PAM sample. Nevertheless, no major physical cell damage or shrinkage was observed in the time-lapse movies.

The mitigation in the number of live MDCK cells at the 48 h time point in the PAM treated sample (compared to the control case) could be the net result of a combination of an increase in the rate of cell death and an inhibition of cell proliferation. To delineate the relative contributions of these factors, the number of dividing cells in the time-lapse sequence was manually counted using ImageJ software and was normalized by the initial total number of cells.
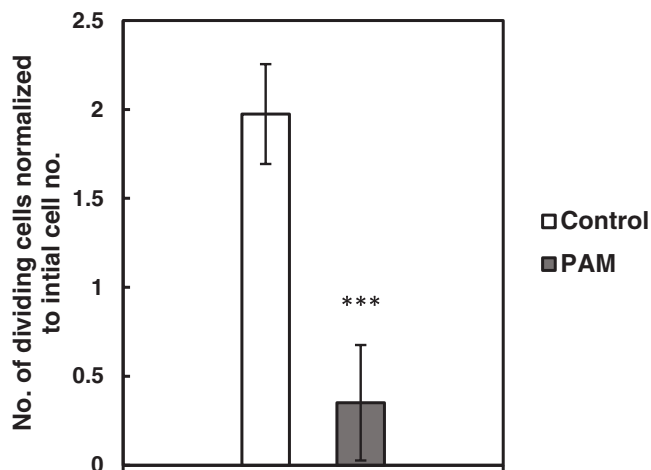


**Figure 5.** Number of division events normalized by initial number of cells in control and PAM as quantified from time-lapse images during 48 h of PAM treatment. Data represent averages from 6 movies from two independent experiments as means ± SD. An independent *t*-test indicates that cell proliferation was significantly lower in PAM treated samples (mean = 1.97, SD = 0.28) than control (mean = 0.40, SD = 0.32), $t(10) = 8.987$, ***$P < 0.001$.

Figure 4 shows an example of a dividing cell in a time-lapse sequence. During mitosis, the cell temporary rounds up, divides into two and the daughter cells re-spread onto the surface. Such cell division events can be clearly seen in our phase time-lapse sequences, as shown in figure 4: the cell
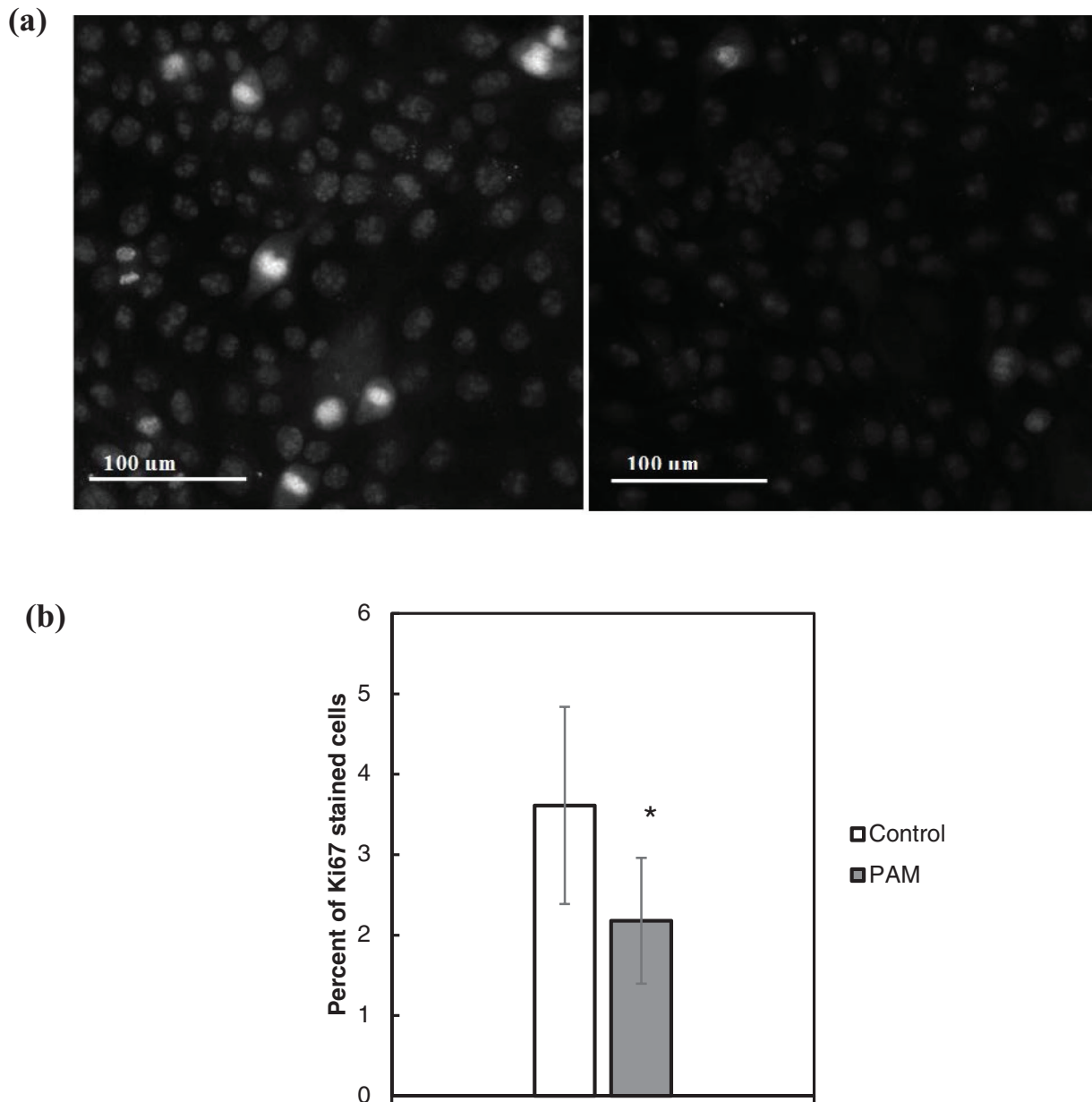
**Figure 6.** (a) Immunofluorescence images of a control (left) and a PAM treated (right) sample, stained for the proliferation marker Ki-67. (b) The average percentage of Ki-67 stained cells in immunofluorescence images in PAM and control samples. Data represent averages from at least eight images from two independent experiments, shown as means $\pm$ SD. *$P < 0.05$ (chi-square test).

morphology changes from being spread to a rounded shape (associated with higher brightness in the periphery) indicating a loss of peripheral focal adhesions [33]. After cell division, daughter cells spread back to recoup their interphase morphology (figure 4). Figure 5 shows the number of division events normalized by the initial number of cells in control and PAM samples. The number of dividing cells was counted in each image sequence acquired from 48 h of time-lapse imaging. This result indicates that cell proliferation was significantly reduced in PAM treated cells ($p < 0.001$) and suggests that mitigation in cell number increase was associated with cell proliferation inhibition.

### 3.3. PAM treatment alters the frequency of Ki-67 nuclear localization in MDCK cells

In order to confirm the inhibition of cell proliferation induced by PAM, the nuclear localization of Ki-67, a marker of cell proliferation, was ascertained using immunofluorescence. Figure 6(a) shows immunofluorescence images from control and PAM treated MDCK cells in which Ki-67 has been stained. Ki-67 staining is markedly brighter in cells that are actively involved in proliferation. The number of Ki-67 stained cells were counted in at least 8 immunofluorescence images obtained with 10× magnification from PAM and control samples. Figure 6(b) shows the percent of Ki-67 stained
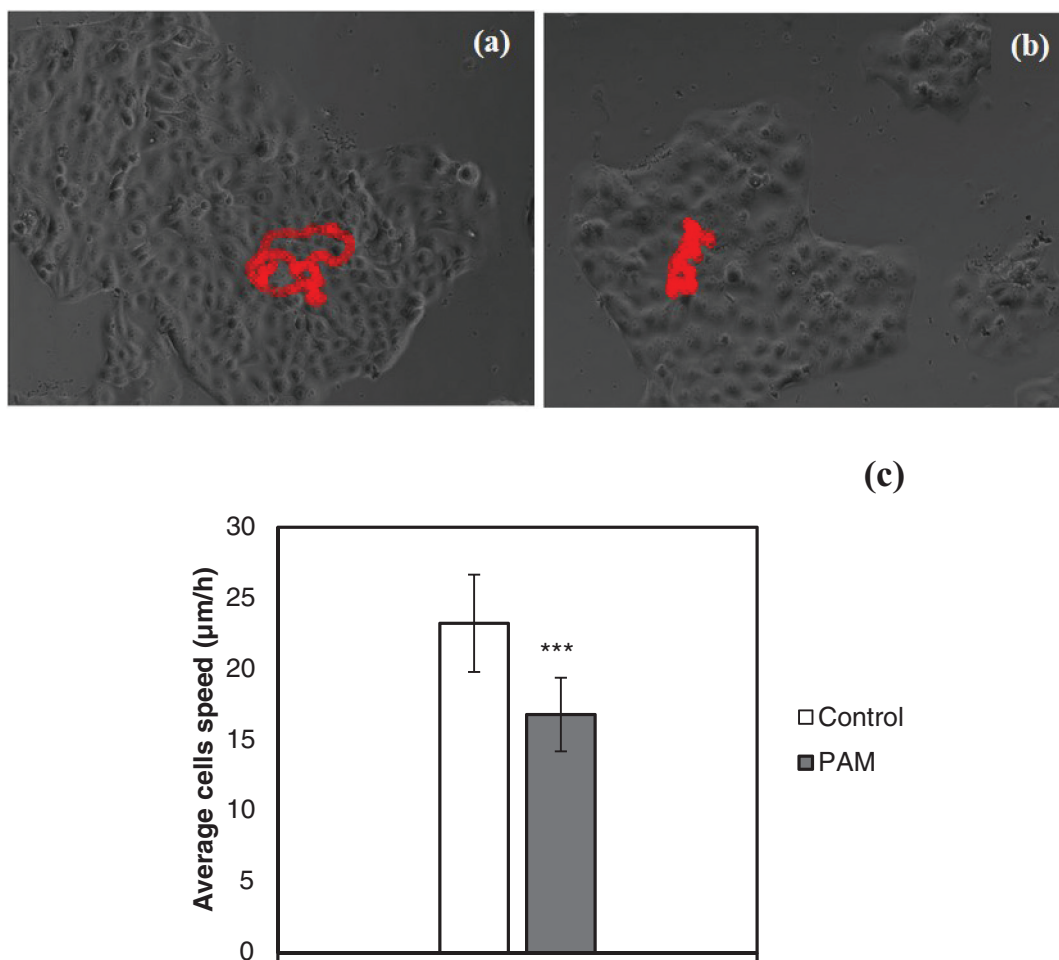
**Figure 7.** Trace of a cell's migration path during time-lapse imaging is shown in red colour in (a) a control sample and (b) a PAM treated sample. (c) The average speed of cells within epithelial islands of PAM and control MDCK samples. Data represent the average in $\mu$m h$^{-1}$ $n = 20$ tracked cells of two independent experiments: means $\pm$ SD. ***$p < 0.001$ (independent *t*-test).

cells, on average, in immunofluorescence images. As shown, the number of Ki-67 stained cells is lower in PAM treated cells than in the control case, which indicates inhibition of proliferation. A chi-square test indicated a significant association between treatment and the number of marked cells, $x^2(1) = 20.53$, $p < 0.05$. In fact, the percentage of stained cells in the control sample was 1.7 times higher than that for the PAM treated cells with a 95% confidence interval of (1.34, 2.11). This result supports the lower rate of cell proliferation in PAM samples as observed using time-lapse imaging.

### 3.4. Effect of PAM treatment on cell migration within cell islands

Time-lapse imaging of MDCK cells upon PAM treatment also suggested that PAM treatment may have affected random cell migration of cells within MDCK islands. To test this quantitatively, single cells within the MDCK islands were tracked in the control and PAM time-lapse sequences using MtrackJ (ImageJ software) and the average speed of single cells was measured (supplementary movies 3 and 4). Figures 7(a) and (b) show the trace of a cell's migration path in control and PAM treated samples, respectively. Figure 7(c) indicates the average speed of single cells in PAM and control samples. This result

indicates that the average cell migration speed of PAM treated cells is lower than that of the control. Results of an independent *t*-test indicated that speed of single cells in PAM treated sample (mean = 16.78 $\mu$m h$^{-1}$, SD = 3.27 $\mu$m h$^{-1}$) is statistically significantly lower than control (mean = 23.23 $\mu$m h$^{-1}$, SD = 3.43 $\mu$m h$^{-1}$), $t(37) = 5.994$, $p < 0.001$. We then performed immunofluorescence experiments to determine if any adverse effects on the actin and adhesion apparatus of MDCK cells underlies the decreased migration speed. Beta-catenin and paxillin (markers of cell–cell and cell-substrate adhesion, respectively) were expressed and distributed similarly in both control and PAM samples. Likewise, the overall filamentous actin organization in the control and PAM treated samples did not differ significantly. These immunofluorescence images are presented in supplementary figures 1–3.

## 4. Conclusion

In this study, the effects of PAM treatment on non-cancerous MDCK epithelial cells were determined using colourimetric assays, time-lapse imaging as well as immunofluorescence staining. While PAM generated with higher time of plasma exposure caused widespread cell death, moderate PAM treatment mitigated the increase in cell number without significant

J. Phys. D: Appl. Phys. **50** (2017) 185205

S Mohades *et al*

cell death. Time-lapse imaging over 2 d of PAM treatment showed that treatment of MDCK cells with PAM created with a moderate time of exposure to LTP resulted in inhibition of cell proliferation. This result was confirmed by immuno-fluorescent localization of Ki-67 in MDCK nuclei. We also found, using tracking of single cells within epithelial cell islands, that PAM treatment decreases the average cell migration speed of MDCK cells. However, both actin and adhesion organization did not differ significantly upon PAM treatment suggesting that PAM treatment impacts part of a cell migration module within these cells. The effects of PAM on epithelial cells addressed in this work has implications in applying LTP directly or through PAM in anti-cancer as well as wound healing applications.

## Acknowledgments

## References

[1] Laroussi M, Tendero C, Lu X, Alla S and Hynes W L 2006 Inactivation of bacteria by the plasma pencil *Plasma Process. Polym.* **3** 470

[2] Navabsafa N, Ghomi H, Nikkhah M, Mohades S, Dabiri H and Ghasemi S 2013 Effect of BCD plasma on a bacteria cell membrane *Plasma Sci. Technol.* **15** 685

[3] Morris A D, McCombs G B, Akan T, Hynes W L, Laroussi M and Tolle S L 2009 Cold plasma technology: bactericidal effects on *Geobacillus stearothermophilus* and *Bacillus cereus* microorganisms *J. Dent. Hyg.* **83** 55

[4] Arndt S *et al* 2013 Cold atmospheric plasma (CAP) changes gene expression of key molecules of the wound healing machinery and improves wound healing *in vitro* and *in vivo PLoS One* **8** e79325

[5] Laroussi M, Mohades S and Barekzi N 2015 Killing adherent and nonadherent cancer cells with the plasma pencil *Biointerphases* **10** 029401

[6] Fridman G, Shereshevsky A, Jost M M, Brooks A D, Fridman A, Gutsol A, Vasilets V and Friedman G 2007 Floating electrode dielectric barrier discharge plasma in air promoting apoptotic behavior in melanoma skin cancer cell lines *Plasma Chem. Plasma Proc.* **27** 163

[7] Barekzi N and Laroussi M 2013 Effects of low temperature plasmas on cancer cells *Plasma Process. Polym.* **10** 1039

[8] Mohades S, Barekzi N and Laroussi M 2014 Efficacy of low temperature plasma against SCaBER cancer cells *Plasma Process. Polym.* **11** 1150

[9] Adachi T, Tanaka H, Nonomura S, Hara H, Kondo S and Hori M 2015 Plasma-activated medium induces A549 cell injury via a spiral apoptotic cascade involving the mitochondrial–nuclear network *Free Radic. Biol. Med.* **79** 28

[10] Kim S J, Chung T H, Bae S H and Leem S H 2010 Induction of apoptosis in human breast cancer cells by a pulsed atmospheric pressure plasma jet *Appl. Phys. Lett.* **97** 023702

[11] Kaushik N K, Uhm H and Choi E H 2012 Micronucleus formation induced by dielectric barrier discharge plasma exposure in brain cancer cells *Appl. Phys. Lett.* **100** 084102

[12] Brullé L, Vandamme M, Riès D, Martel E, Robert E, Lerondel S, Trichet V, Richard S, Pouvesle J M and Le Pape A 2012 Effects of a non thermal plasma treatment alone or in combination with gemcitabine in a MIA PaCa$_2$-luc orthotopic pancreatic carcinoma model *PLoS One* **7** e52653

[13] Wende K *et al* 2015 Identification of the biologically active liquid chemistry induced by a nonthermal atmospheric pressure plasma jet *Biointerphases* **10** 029518

[14] Lu X, Naidis G V, Laroussi M, Reuter S, Graves D B and Ostrikov K 2016 Reactive species in non-equilibrium atmospheric-pressure plasmas: generation, transport, and biological effects *Phys. Rep.* **630** 1

[15] Yan X, Xiong Z, Zou F, Zhao S, Lu X, Yang G, He G and Ostrikov K 2012 Plasma-induced death of HepG2 cancer cells: intracellular effects of reactive species *Plasma Process. Polym.* **9** 59

[16] Zhang C, Walker L M and Mayeux P R 2000 Role of nitric oxide in lipopolysaccharide-induced oxidant stress in the rat kidney *Biochem. Pharmacol.* **59** 203

[17] Arjunan K, Sharma V and Ptasinska S 2015 Effects of atmospheric pressure plasmas on isolated and cellular DNA—a review *Int. J. Mol. Sci.* **16** 2971

[18] Laroussi M 2014 From killing bacteria to destroying cancer cells: 20 years of plasma medicine *Plasma Process. Polym.* **11** 1138

[19] Ratovitski E A, Cheng X, Yan D, Sherman J H, Canady J, Trink B and Keidar M 2014 Anti-cancer therapies of 21st century: novel approach to treat human cancers using cold atmospheric plasma *Plasma Process. Polym.* **11** 1128

[20] Zucker S N, Zirnheld J, Bagati A, DiSanto T M, Des Soye B, Wawrzyniak J A, Etemadi K, Nikiforov M and Berezney R 2012 Preferential induction of apoptotic cell death in melanoma cells as compared with normal keratinocytes using a non-thermal plasma torch *Cancer Biol. Ther.* **13** 1299

[21] Horwitz R and Webb D 2003 Cell migration *Curr. Biol.* **13** R756

[22] Stoffels E, Kieft I E, Sladek R E J, van den Bedem L J M, van der Laan E P and Steinbuch M 2006 Plasma needle for *in vivo* medical treatment: recent developments and perspectives *Plasma Sources Sci. Technol.* **15** S169

[23] Shashurin A, Stepp M A, Hawley T S, Pal-Ghosh S, Brieda L, Bronnikov S, Jurjus R A and Keidar M 2010 Influence of cold plasma atmospheric jet on surface integrin expression of living cells *Plasma Process. Polym.* **7** 294

[24] Kim C H, Bahn J H, Lee S H, Kim G Y, Jun S I, Lee K and Baek S J 2010 Induction of cell growth arrest by atmospheric non-thermal plasma in colorectal cancer cells *J. Biotechnol.* **150** 530

[25] Shashurin A, Keidar M, Bronnikov S, Jurjus R A and Stepp M A 2008 Living tissue under treatment of cold plasma atmospheric jet *Appl. Phys. Lett.* **93** 181501

[26] Plewa J M, Yousfi M, Frongia C, Eichwald O, Ducommun B, Merbahi N and Lobjois V 2014 Low-temperature plasma-induced antiproliferative effects on multi-cellular tumor spheroids *New J. Phys.* **16** 043027

[27] Mohades S, Barekzi N, Razavi H, Maruthamuthu V and Laroussi M 2016 Temporal evaluation of the anti-tumor efficiency of plasma-activated media *Plasma Process. Polym.* **13** 1206

[28] Wang M, Holmes B, Cheng X, Zhu W, Keidar M and Zhang L G 2013 Cold atmospheric plasma for selectively ablating metastatic breast cancer cells *PLoS One* **8** e73741

[29] Iseki S, Nakamura K, Hayashi M, Tanaka H, Kondo H, Kajiyama H, Kano H, Kikkawa F and Hori M 2012 Selective killing of ovarian cancer cells through induction of apoptosis by nonequilibrium atmospheric pressure plasma *Appl. Phys. Lett.* **100** 113702

J. Phys. D: Appl. Phys. **50** (2017) 185205

S Mohades *et al*

[30] Fridman G, Friedman G, Gutsol A, Shekhter A B, Vasilets V N and Fridman A 2008 Applied plasma medicine *Plasma Process. Polym.* **5** 503

[31] Graves D B 2012 The emerging role of reactive oxygen and nitrogen species in redox biology and some implications for plasma applications to medicine and biology *J. Phys. D: Appl. Phys.* **45** 263001

[32] Laroussi M 2015 Low-temperature plasma jet for biomedical applications: a review *IEEE Trans. Plasma Sci.* **43** 703

[33] Cramer L P and Mitchison T J 1997 Investigation of the mechanism of retraction of the cell margin and rearward flow of nodules during mitotic cell rounding *Mol. Biol. Cell.* **8** 109